PriMera Scientific Engineering
Volume 4 Issue 5 May 2024
ISSN: 2834-2550

PriMera Scientific Publications

Nonlinear Detection in Wave Loaded Structures

Type: Review Article
Received: March 22, 2024
Published: April 26, 2024

Citation:
Rune Brincker., et al. "Nonlinear Detection in Wave Loaded Structures". PriMera Scientific Engineering 4.5 (2024): 34-41.

Rune Brincker[1]*, Sandro Amador[2] and Ruben Boroscheck[3]

[1]*Brincker Monitoring ApS, Denmark*

[2]*Technical University of Denmark (DTU), Denmark*

[3]*University of Chile, Chile*

***Corresponding Author:** Rune Brincker, Brincker Monitoring ApS, Denmark.

Abstract

When steel structures experience short duration overloads, for instance wind burst or a breaking wave, the structure might yield for a short moment and after this yielding event the reduction of stiffness could be minimal. The result is mainly a permanent deformation, which is normally detected using tilt meters. But since tilt meters are measuring angles at the location of instrumentation, and in some cases, yielding does not result in permanent changes of tilt angles, the yielding must in these cases be detected by other means. In this paper we are shortly discussing the use of the short duration changes of natural frequency and damping following ideas from the earthquake cases of period elongation. However, due to the strong influence of the external forces on the estimation of these changes, other effects are considered such as quasistatic displacement movement, slamming effect of the overload, permanent displacement using low frequency signals, and mode shape changes using principles from stochastic subspace identification. This defines a set of five non-linear detection (NLD) indicators that are studied on a case of possible yielding in a wave loaded offshore structure using simulation.

Keywords: Short duration overload; permanent deformation; quasistatic displacement; Bloop; SSI null space; wave loading; offshore structure

Introduction

Wave loads are difficult to prescribe due to the uncertainty on the behavior of the wave that can be influenced by steepness, that is the ratio of wave height to length. If the steepness exceeds a certain value, the wave might break and result in significant larger forces than the classical linear wave.

If structures are loaded by breaking waves, the time dependence of the loading force is very different from the loading produced by the linear waves. The breaking wave normally has a short and large force action including a good deal of impact, see [1-3]. Therefore, in this paper, we are restricting the evaluation to a single yield due to the dominant breaking wave.

In this paper we will consider how the permanent deformations of an offshore structure can be estimated using a classical structural health monitoring (SHM) system consisting of classical sensors like accelerometers mounted on the topside of the considered structure.

Classical measures of permanent deformation

When a structure is overloaded damage can occur. This damage typically produces a temporally or permanent change of its tangential stiffness and residual displacement at local or global level.

Temporally yielding in steel structure presents a challenge for detection and quantification. Assuming a single yielding episode the initial and final stiffness in stable steel systems are nearly the same, limiting the capacity for detection associated with stiffness parameters outside the short time of yielding. The yielding could be detected by strain sensors located in the yielding region. This is possible only when the structure has been designed to have specific areas of yielding or a very precise model and loading is available, so location of yielding can be predicted. Another possibility is to detect this yielding by its consequences on the overall residual displacement of the system. This requires that the local yielding has a detectable effect on the overall displacement.

The global permanent deformation could be translational, rotational or a combination of both. Noting that offshore steel platforms are far away from any fixed reference, so monitoring relative motion is not possible. We must rely on inertial or absolute measurement. Direct measurements using GPS system is not reliable enough to detect small motions. To try to capture residual displacement, translational accelerometers need to have high sensitivity at DC and low frequency, but this measurement is strongly affected by any rotation (permanent or temporary) that affects the sensor. A tilt meter is an option if the damage generates a rotation at the position of the tilt meter location.

Tilt meters have well-known quality of producing reliable DC values of the tilt. This will work well if the failure mechanism in the structure has a global expression, for example tension failure in the legs or in the foundation, but if we consider failure in a diagonal of a jacket offshore structure, the failure mechanism may mainly produce a permanent angle around the vertical axis, and thus no signal might be detected by the tilt meter.

During the yielding process a change (reduction) of the tangent stiffness occurs. This change of stiffness could be detected by localized time frequency identification. The shorter the duration of the yielding period, the more difficult its detections. On reinforced concrete structure damage causes a permanent stiffness change that can easily be detected by monitoring post yielding vibrations, this is not necessary for the case of steel structures. Localize yielding has been detected by identifying temporary modal parameter changes using Short Time Fourier Transform and Short Time System Identification, see [4].

Proposed indicators

We will formulate and investigate the following indicators for permanent deformation: the maximum deformation estimated by integrating acceleration, the slamming force estimated from the change of system energy, the low frequency signal below the peak value of the wave spectrum that is increasing during development of permanent deformation, and finally we will use the idea of the null space defined by Stochastic Subspace identification (SSI) damage detection technique that will define two indicators. Thus, in the following we will give a short introduction to the so defined five indicators for permanent deformation due to short duration yielding in the structure.

Maximum displacement indicator

It is the maximum quasistatic displacement that is chosen to be the basic key indicator. The idea is that the owner of the considered offshore platform perform a series of simulations, including simulation of the total platform response using a reasonable wave model with different kinds of breaking wave models, so that some of the simulation cases will experience yielding. Thus, this kind of simulation requires both a nonlinear and realistic wave model and a similarly non-linear and realistic finite element (FE) model of the total

structure.

Based on these simulations, the cases will be divided into two sets of simulation cases

- Cases without yielding,
- Cases with yielding.

and based on these results for each wave direction, a critical value for the maximum displacement is defined as explained in the following.

Let the acceleration signals from several sensors spatially distributed at the top side be contained in the response vector $\ddot{\mathbf{y}}(t)$, so that the responses can be integrated to produce the displacement response vector $\mathbf{y}(t)$, for instance using integration as defined in [4-7].

Using the response locally around the time of the event of the critical wave hitting the structure, the covariance matrix $\mathbf{C}$ can be estimated, and decomposed by SVD to produce the dominating singular vector $\mathbf{u}$, so that the principal response can be estimated.

$$y_p(t) = \mathbf{u}^T \mathbf{y}(t) \quad (1)$$

This defines the 1DOF response for each event and the corresponding principal direction defined by the dominating horizontal response of the singular vector $\mathbf{u}$, restricting our evaluation to yielding that have expression mainly on the horizontal global motions.

Based on the principal response that should also include the quasistatic displacement, we can then define the corresponding maximum quasistatic displacement as the primary damage indicator.

$$d_1 = \max\left(\mathbf{u}^T \mathbf{y}(t)\right) \quad (2)$$

Based on this damage indicator the critical displacement can then be defined based on the above mentioned classification and classical safety analysis to be defined as the quantity y_c. However, we do not further discuss how reliability principles should be used to arrive at the appropriate critical value for the damage indicator d_1, since it is not the focus of this paper.

In the following we will consider the platform as a SDOF system with the displacement $u(t) = y_p(t)$, the velocity $v(t) = \dot{y}_p(t)$, and the acceleration $a(t) = \ddot{y}_p(t)$ with the SDOF mass m and stiffness and k respectively.

Slamming force indicator

To obtain an indicator of the slamming force from the breaking wave, we consider the derivative of the energy here neglecting the damping force.

$$\begin{aligned} \dot{E}(t) &= \frac{d}{dt}(mv^2(t) + ku^2(t))/2 \\ &= mv(t)a(t) + ku(t)v(t) \\ &= (ma(t) + ku(t))v(t) = F(t)v(t) \end{aligned} \quad (3)$$

where *F(t)* is the external force on the 1DOF system. Thus, we see that this indicator is attractive because it is proportional to the wave force *F(t)* times the velocity *v(t)*, and both high force and high velocity are indicators of a dangerous event. An easy way to calculate the indicator is to use the Hilbert Transform to obtain the envelope *e(t)* of *u(t)* and use that the energy is then given by $E(t) = ke^2(t)/2$ so that the slamming indicator can be obtained as.

$$d_2 = \max\left|\dot{E}(t)\right| = \max\left|ke(t)\dot{e}(t)\right| \quad (4)$$

Bloop indicator

This indicator is meant to provide a direct measure of the permanent deformation that we can think of as being proportional to a Heaviside step function *H*(*t*), so that we can define the permanent deformation as a function of time as.

$$u(t) \propto \Delta u H(t) \quad (5)$$

It is well known that *H*(*t*) is the integral of the Dirac delta function $\delta(t)$, so that since the spectral density of $\dot{u}(t)$ then is flat, according to the integration theorem of the Fourier transform, the corresponding spectral density of $u(t)$ is then proportional to $\Delta u / \omega^2$. This means that close to DC we will see a high increase in the LF noise during the short moment of the development of the permanent deformation.

The increase of the LF noise can be observed using a narrow band pass filter below the peak frequency value ω_p of the wave spectrum. This works when the LF noise produced by the waves below ω_p is rather limited, and when integration noise close to DC can be avoided to play a significant role. In the following investigations we used the following frequency interval for the LF bandpass filter.

$$I = [\omega_p / 4; \omega_p / 2] \quad (6)$$

If the band pass filter is given by the linear operator $O_I\{.\}$, then the bloop damage indicator is defined as.

$$d_3 = \max \left| O_I\{u(t)\} \right| \quad (7)$$

SSI Indicators

Finally, we will consider the SSI damage detection technique formulated 10-15 years ago, see [9-10]. This technique is based on the principle of defining the physical subspace as the modal subspace, and everything that falls out of the physical subspace as the so-called null-space defining components indicating damage.

Following this idea, we can define the part of the response that belong to the null-space as $\mathbf{y}_n(t)$. Let us assume that the null space response measured by the sensors can be described as a rigid body movement, so that.

$$\mathbf{y}(t) = \mathbf{T}\mathbf{b}(t) \quad (8)$$

where **T** is a full rank transformation matrix (rank 6), and ***b***(*t*) is the rigid body deformation vector made by stacking the translation vector ***t***(*t*) containing the translation components in the directions of the coordinate system and the rotation vector ***r***(*t*) containing the rotation angles around the coordinate axis's. The part of the null space $\mathbf{y}_n(t)$ that can be considered as not dominated by measurement noise, can be written in the same form.

$$\mathbf{y}_n(t) = \mathbf{T}\mathbf{b}_n(t) \quad (9)$$

and the corresponding rigid body vector can be estimated as.

$$\hat{\mathbf{b}}_n(t) = \mathbf{T}^{+}\mathbf{y}_n(t) \quad (10)$$

where $\mathbf{T}^{+}$ is the pseudo inverse of **T**. Since we are assuming that sensors are mounted only on the topside of the structure, the physical part of the null space response will be rigid body motion, and since the magnitude of the translation does not matter but only the shape, the null space movement will be dominated by rotation only. We will divide the rotational response into two components, the principal rotational movement, and the compression of the neutral axis.

The null space rotation is the rotation that does not belong to the first principal vector, which should be considered as the current mode shape of the structure, and should therefore be considered as a non-linear component. Thus, the corresponding SSI indicator d_4

is the null space deformation projected onto the principal direction given by Eq. (1).

$$d_4 = \max\left|\mathbf{u}^T \mathbf{T}\hat{\mathbf{b}}_n(t)\right| \quad (11)$$

The compression is the part of the rotation that can be interpreted as a compression of the axis that describes the neutral axis of the offshore jacket structure, normally the vertical middle axis of the structure, see Figure 1.

If the compression of the axis is $c(t)$, the final SSI indicator d_5 is then given by.

$$d_5 = \max\left|c(t)\right| \quad (12)$$

Simulation case

30 data sets were simulated with 4 3D sensors mounted in the corners of the top side, see Figure 1. Figure 2 shows the horizontal displacement results of integrating once the velocity and twice the acceleration time histories using one of the considered data sets. As we can observe, the resulting principal displacement signals derived from velocity or acceleration are close to identical.

Running the 30 data sets through the above-mentioned algorithms for the NLD indicators we will obtain 30 values for each of the indicators $d_i(n)$, n running from 1 to 30. Collecting the five NLD indicators in the damage vector.

$$\mathbf{d}(n) = \left\{d_1(n), d_2(n), d_3(n), d_4(n), d_5(n)\right\}^T \quad (13)$$

providing the initial (raw) date that comes from each of the indicator algorithms. However, in order to provide a more meaningful set of signals, each of indicators $d_i(n)$ are normalized with respect to its mean values.

$$\mu_i = E\left[d_i(n)\right] \quad (14)$$

where $E\left[d_i(n)\right]$ is the mean over the 30 data sets. This produces the dimensionless and normalized damage indication vector.

$$\mathbf{d}_0(n) = \left\{d_1(n)/\mu_1, d_2(n)/\mu_{12}, d_3(n)/\mu_3, d_4(n)/\mu_4, d_5(n)/\mu_5\right\}^T \quad (15)$$

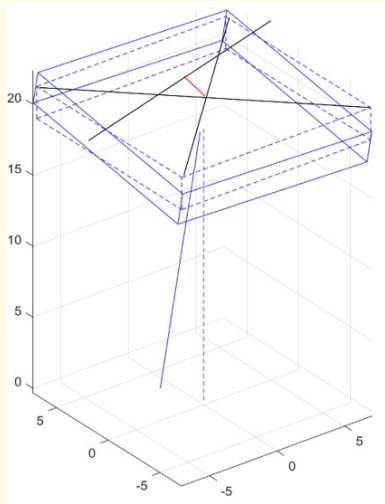

Figure 1: Example of rotation in the null-space according to the SSI damage detection for data set 21. The red line indicates the distance of the rotation line to the neutral axis, thus indicates a compression of the neutral axis which is an indication of damage.

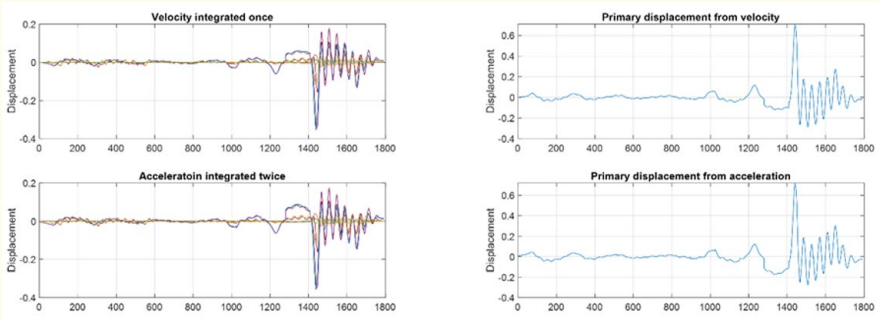

Figure 2: Example of results of integrating velocity and acceleration and projecting on the principal direction as defined in Eq. (1). Left: all sensor signals integrated, right: Principal displacement.

If we now multiply this damage indication vector with previous mentioned critical displacement y_c, all the indicators will now be an estimate of the critical displacement. Each of the indicators now should be considered as stochastic variable estimating displacement that represents an estimate of the critical displacement.

In the considered example using the 30 simulated data sets, no reliability considerations have been made, and the mean values has only been multiplied by a factor 1.2 in order roughly to introduce a safety factor. The alarm levels based on the indicators have then been defined as shown in Table 1, that also shows the classification values for different alarm settings.

The true indication of damage has been obtained from the simulations, and the similar results based on yielding strains are shown in Table 2.

Studying the results, we can observe the following

- "Dark red" strain indications are either the same or "Red" for the indicators.
- "Red" strain indications are either the same or "Dark red" for the indicators.
- "yellow" strain indications are not the same as the indications, but are all either "Dark red", "Red" or "Green".
- "Green" strain indications are either the same or "yellow" or "Red" for the indicators.

In Table 1 and 2 the classifications that are the same for the true classification and classification estimated by the NLD indicators are marked in bold. Note that the scale is different because the true damage is given in terms of yielding train, and the indicators are given in terms of the normalized value multiplied by the factor 1.2.

The only two indication results that can be said to be misleading are for the datasets 13 and 21. For data set 13 the indicators say, "Dark red", but the strain say "yellow", and for the data set 21 the indicators say "Red" but the strain say "Green". Both for data set 13 and 21 the misleading information is on the safe side. One can say that the only real "false Red" was for data set 21.

The only indicator information on the un-safe side are the data from data sets 19 and 20 where the indicators say "Green" and the strain say "yellow".

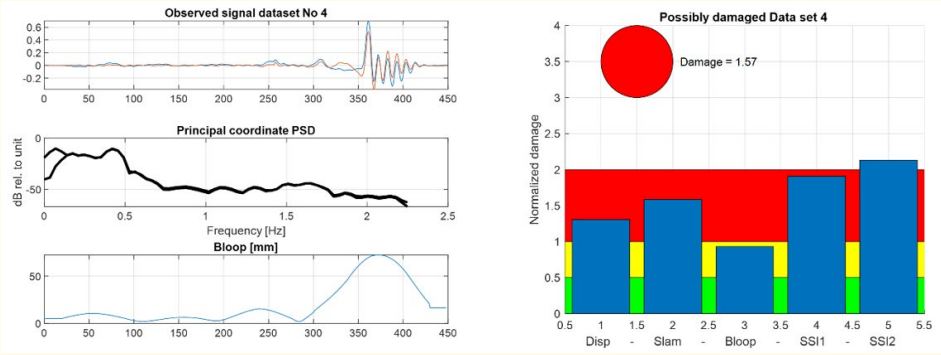

Figure 3: Typical analysis results and the alarm signal for data set 4. Left top plot, blue signal is the principal displacement using full simulated frequency band and red signal is the principal signal using the quasistatic high pass filter that only includes the peak of the wave spectrum around 0.15 Hz. Left middle plot: spectral densities for the two filters, Left bottom plot: Estimated Bloop signal for damage indicator 3. Right: The five defined alarm signals showing the value of the defined damage indicators d_1 to d_5 from the left to the right.

Classification	***Dark red***	***Red***	***Yellow***	***Green***
Indicator range	>1.5	>1.0	0.5-1.0	0-0.5
Data sets	13, **16, 18**, 25, 29	**1**, 2, **3, 4, 5, 7**, 8, 9, **10**, 11, 12, **14**, 15, 17, 21, 23, 24, **26, 28, 30**	22, 27	**6**, 19, 20

Table 1: Results of using the NLD indicators.

Classification	***Dark red***	***Red***	***Yellow***	***Green***
Strain range [%]	>4.5	0.3-4.5	0-0.3	0
Data sets	8, 11, 12, 15, **16, 18**, 24	**1, 3, 4, 5, 7, 10**, **14**, 25, **26, 28**, 29, **30**	2, 9, 13, 17, 19, 20	**6**, 21, 22, 27

Table 2: Results of considering yielding strains from the response simulation.

Conclusions

Five damage indicators have been defined that are all estimates of the principal displacement in the principal direction but based on the following principles:

1. Displacement obtained by integration of acceleration.
2. Slamming measure based on energy raise.
3. Bloop from the LF region below the peak frequency of the wave spectrum.
4. SSI based null space quantity based on added rotation of the topside.
5. SSI based null space quantity based on compression of the neutral axis.

Comparing the results of the indicators with the strain result from the simulations show that only in two of the 30 simulation cases the indicators fail to provide information that provide minor misleading information on the unsafe side.

In this investigation is only given an initial presentation of the defined damage indicators. We have not made an evaluation of how much yielding we can detect and similar issues. Noise in real applications will affect the indicators, which might dimmish their value.

Also, it is needed to test the so defined indicators in a larger set of data ranging over the whole range of responses from many linear responses to a limited number of non-linear responses, and then illustrate to what degree the indicators can provide meaningful information about the non-linear events.

Acknowledgements

The work has been supported by the Danish foundation "Innovation Fund Denmark" in the InnoSHM project under the reference number 0175-00028B.

References

1. Cuomo Giovanni., et al. "Breaking wave loads at vertical seawalls and breakwaters". Journal of Coastal Engineering 57.4 (2010).
2. Tychsen Jesper and Martin Dixen. "Wave kinematics and hydrodynamic loads on intermediate water depth structures inferred from systematic model testing and field observations - Tyra Field Extreme Wave Study 2013-15". Proc. of the 3rd Offshore Structural Reliability Conference, OSRC2016, 14-16 September, Stavanger, Norway (2016).
3. Tychsen Jesper., et al. "Summary of the impact on structural reliability of the findings of the Tyra Field Extreme Wave Study 2013-15". Proc. of the 3rd Offshore Structural Reliability Conference, OSRC2016, 14-16 September, Stavanger, Norway (2016).
4. Boroschek R and Santos JP. "Civil Structural Testing". In Handbook of Experimental Structural Dynamics". Springer New York (2020): 1-95.
5. Akkar Sinan and David M Boore. "On Baseline Corrections and Uncertainty in Response Spectra for Baseline Variations Commonly Encountered in Digital Accelerograph Records". Bulletin of the Seismological Society of America 99.3 (2009): 1671-90.
6. Boroschek RL and D Legrand. "Tilt Motion Effects on the Double-Time Integration of Linear Accelerometers: An Experimental Approach". Bulletin of the Seismological Society of America 96.6 (2006).
7. Kaya Yavuz and Erdal Safak. "Real-Time Analysis and Interpretation of Continuous Data from Structural Health Monitoring (SHM) Systems". Bulletin of Earthquake Engineering 13.3 (2015): 917-34.
8. Brandt Anders and Rune Brincker. "Integrating time signals in frequency domain - Comparison with time domain integration". Journal of Measurement (2014).
9. Döhler, Michael, Laurent Mevel and Falk Hille. "Subspace-Based Damage Detection under Changes in the Ambient Excitation Statistics". Mechanical Systems and Signal Processing 45.1 (2014): 207-224.
10. Viefhues, Eva., et al. "Stochastic Subspace-Based Damage Detection with Uncertainty in the Reference Null Space". IWSHM - 11th International Workshop on Structural Health Monitoring, Stanford (2017).